PERFORMANCE OF SOLAR DRYER CHAMBER USED FOR CONVECTIVE DRYING OF SPONGE-COTTON

by

Walid AISSA[a*], Mostafa El-SALLAK[b], and Ahmed ELHAKEM[a]

[a] Mechanical Power Department, High Institute of Energy, South Valley University, Aswan, Egypt
[b] Mechanical Power Engineering Department, Faculty of Engineering, Cairo University, Cairo, Egypt

Original scientific paper
DOI: 10.2298/TSCI110710084A

Solar dryer chamber is designed and operated for five days of July 2008. Drying experiments are conducted for sponge-cotton; as a reference drying material in the ranges between 35.0 to 49.5 °C of ambient air temperature, 35.2 to 69.8 °C drying air temperature, 30 to 1258 W/m^2 solar radiation, and 0.016 to 0.08 kg/s drying air flow rate. For each experiment, the mass flow rate of the air remained constant throughout the day. The variation of moisture ratio, drying rate, overall dryer efficiency, and temperature distribution along the dryer chamber for various drying air temperatures and air flow rates are discussed. The results indicated that drying air temperature is the main factor in controlling the drying process and that air mass flow rate has remarkable influence on overall drying performance. For the period of operation, the dryer attained an average temperature of 53.68 °C with a standard deviation of 8.49 °C within a 12 h period from 7:00 h to 19:00 h. The results of this study indicated that the present drying system has overall efficiency between 1.85 and 18.6% during drying experiments. Empirical correlations of temperature lapse and moisture ratio in the dryer chamber are found to satisfactorily describe the drying curves of sponge-cotton material which may form the basis for the development of solar dryer design charts.

Key words: *dryer chamber, moisture ratio, drying rate, overall efficiency, empirical correlations*

Introduction

The principal aim in a drying operation is the supply of heat required to provide the best product quality with minimum energy consumption. There are two techniques for drying of food staff, leather and clothes, namely, open sun drying and solar drying in a drying system. In solar drying, air heaters utilize the heat collected from solar radiation to supply the thermal energy to the drying air [1-3]. The heated air is then ducted to a thermally and well-insulated dryer chamber [4, 5] to dry the product before expelling to the atmosphere through solar chimney.

The purpose of a dryer is to supply the product with heat by conduction and convection from the surrounding air more than that available under ambient conditions at temperatures above that of the product, or conduction from heated surfaces in contact with the product [4, 5]. The solar chimney is used to regulate the residency period of the drying air within the drying chamber, increase the overall efficiency of the dryer and thermo-siphoning of air (in the case of free convection) and maintain optimum temperature inside the dryer chamber with better circulation of air (in the case of forced convection) which prevent excessive increase of the temperature inside the dryer chamber and adverse effects on the quality of the dried product.

* Now at Faculty of Engineering, Rabigh, King Abdulaziz University, KSA
Corresponding author; e-mail: walidaniss@gmail.com

Heat absorbed by the product supplies the energy necessary for the vaporization of water from the surface of the product. When the absorbed energy has increased to the limit that water vapor pressure of the product moisture will be higher than the vapor pressure of the surrounding air, water from the surface of the moist product starts to vaporize. This leads to a subsequent decrease in the relative humidity of the drying air, increasing its moisture carrying capacity and ensuring a sufficiently low equilibrium moisture content [4, 5]. The nature of the product and its moisture content greatly affect the process of moisture immigration to the surface.

Although economic aspects necessitates maximum drying rates, however the product quality must be considered [4, 6]. Some physical properties of the product to be dried (size, density, *etc.*), moisture content and mass-heat transfer coefficients between the air and the product, all vary during the drying process. Further, drying process is affected by the conditions external to the product such as temperature, humidity and mass flow rate of the drying air and also by changes in the chemical composition of the product to be dried (if any). Temperature of the drying air is a critical factor which affects the drying process. Maximum allowable temperature will exist for each product. This temperature is usually 15-20 °C higher than the ambient temperature [7, 8]. If the surrounding air is humid, then drying will be slowed down. Increasing the air flow, however, speeds up the process by moving the surrounding moist air away from the product. So, a well-designed solar dryer implies utilizing maximum solar energy and producing maximum air flow rate while maintaining the optimum temperature inside the dryer.

A lot of experimental and theoretical investigations have been conducted for the technical aspects and development of various types of solar dryer chambers [9].

Shanmugam and Natarajan [10] designed and fabricated an indirect forced convection and desiccant integrated solar dryer to investigate its performance under the hot and humid climatic conditions of Chennai, India. The system consisted of a flat plate solar air collector, drying chamber, and a desiccant unit. They performed drying experiments for green peas at different air flow rates. The variation of $\ln\varphi$ with drying time, t, was used to calculate the drying constant, k. The drying constant for green peas was obtained from the experimental results and then correlated with drying product temperature, T_g. Linear correlation was found to fit between k and T_g.

Kadam and Samuel [11] developed and tested a forced convective, flat-plate, solar heat collector for drying cauliflower. Ambient and collector outlet air temperature as well as relative humidity (*RH*) were measured at an interval of 1 h for 28-day experimental period. The temperature rise of the drying air ranged from a minimum of 1.7 °C to a maximum of 13.5 °C and the *RH* reduction was from a minimum of 1.59% to a maximum of 10.5% by passing through the solar collector at a mass flow rate of 4.81 m^3/s. The average midday thermal efficiency was around 16.5%. A linear correlation between the temperature difference from ambient ($T - T_a$) and the radiation I, as well as inlet and outlet air temperature and *RH* were obtained. The relation between moisture ratio and drying time was found and drying constant, k, was calculated.

In our previous work [12], we constructed and experimentally and analytically investigated forced convection flat plate solar air heater with granite stone storage material bed in five clear sunny days of July 2008 under the climatic conditions of Aswan, Egypt. The effects of varying air mass flow rate on air heater performance were discussed. Temperature distributions were presented in non-dimensional form. The variation of solar radiation, air heater efficiency, Nusselt number, and temperature distribution along the air heater were dis-

cussed. In addition, comparisons between the calculated values of outlet air temperatures, average air temperatures and storage material temperatures and the corresponding measured values were made and showed good agreement.

Situated near the equator, Aswan governorate receives relatively high solar radiation. Consequently, the utilization of a solar drying technology is considered to be an alternative solution to the problem of drying agricultural products in this governorate. The literature reviews reveal that a comprehensive procedure for evaluating the performance of solar dryer chamber utilized for drying of sponge-cotton material is not available. The main objective of the current work is to design, construct and experimentally investigate the performance of solar dryer chamber in specific meteorological site (Aswan city, Egypt) with (N23°58′ and E32°47′) utilized for drying of sponge-cotton material under different operating conditions in five testing days in July 2008. During the test, air flow rates are 0.08, 0.064, 0.048, 0.032, and 0.016 kg/s, and temperature varies from 35.2 to 69.8 ºC. The experimental results are compared with those in previous investigation in order to verify and monitor how this may predict the experimental results obtained. Empirical values of temperature decay across dryer chamber and moisture ratio determined from the drying experiments may be employed for calculating the system thermal performance.

Description of tested solar dryer chamber

The experimental test rig used in the present work is shown in fig. 1.

The dryer chamber outer dimensions are 1.0 × 0.6 × 1.2 m^3. It is fabricated from wood. A painted black cylindrical hollow chimney, made from galvanized iron, of 0.4 m height and 0.1 m diameter is connected to the top of the drying chamber. A V-shaped aluminum cap (0.2 m wide) is placed at the top of the chimney to protect the dryer from foreign objects. There is a clearance between the chimney and the cap of 0.08 m to allow warm humid air to exit freely from the dryer.

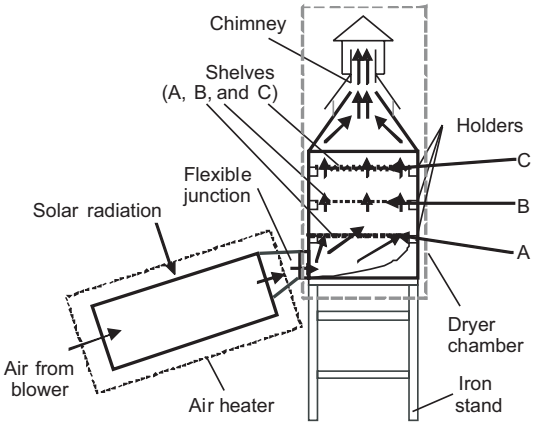

Figure 1. Schematic diagram of test rig

Due to the high air resistance encountered when forcing the air through the drying product, only a few numbers of drying shelves can be stacked without significantly affecting the air movement [6]. Three drying shelves forming three horizontal planes, A, B, and C, fig. 2, are made from wire meshes fixed on wooden frames with dimensions (0.9 m × 0.5 m) to carry the drying material. The drying shelves are kept on the wooden frame fixed to the inner side walls of the drying chamber and can be easily removed to load or unload the drying product from the door, which represents one side of the drying chamber. The bottom shelf A is located 0.35 m above the drying chamber's base; (hot air's entry point). The middle shelf B is placed 0.6 m and the top shelf C is 0.85 m above the chamber's base. The shelves are kept apart from each other to ensure a uniform air circulation under and around the drying material. Wire mesh is also placed at the inlet of the drying chamber for uniform distribution of air in the drying chamber.

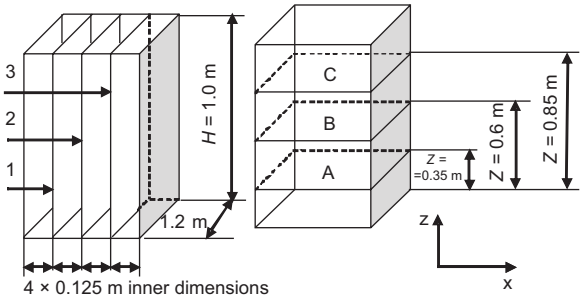

Figure 2. Layout of the relative position of the shelves inside the drying chamber (not in scale)

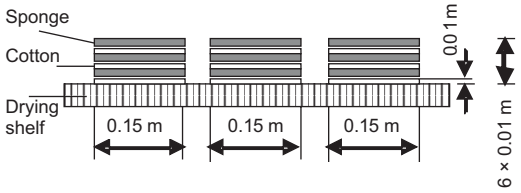

Figure 3. Sponge-cotton specimens loaded in drying shelves

As shown in fig. 2, the drying chamber is divided into three vertical virtual planes, (1), (2), and (3) called section 1, section 2, and section 3. In order to minimize thermal losses due to conduction and convection, *etc.* the drying chamber is well insulated from all four sides. The air heater is connected to the drying chamber through a flexible insulated junction, fig. 1.

Twelve sponge-cotton specimens, fig. 3, each having 0.2 m × 0.15 m × × 0.06 m dimensions and 1.25 kg dry mass is put in each shelf. Specimens are uniformly spread evenly on each drying shelf.

A calibrated hygro-thermometer (YF--180) having K(CA)NiAI/NiCr thermocouple TP-02 type of –50 °C to 1300 °C measuring range, resolution = 1 °C and accuracy = ±(0.5 %, +1 °C), is used to measure the temperature at various locations of the system. All thermocouple junctions exposed to solar radiation are covered with a thin aluminum foil in order to diminish the errors resulting from the solar radiation absorbed by the thermocouple junctions. The measuring probes are inserted through the holes opened at the two side walls of the chamber. The positions of these holes are arranged in the three horizontal levels; A, B and, C and the three vertical planes, 1, 2, and 3. Local measured data of global solar radiation incident on a horizontal surface on July 2, 3, 4, 5, 6, 2008 (testing days) obtained by direct contact with Egyptian meteorological authority is utilized in this work [12]. An electronic balance of 0.001 g accuracy is used to measure the mass loss of the product during the drying process. The mass flow rate of air is measured using calibrated Pitot tube.

Experimental procedure

Experiments are conducted to study many important performance parameters of solar dryer chamber such as moisture ratio, drying rate and overall system drying efficiency. Drying experiments are conducted outdoors for different five days in July 2008 during the summer season. Sponge-cotton material is used as a reference drying material to study the effects of mass flow rate as well as the climatic and operational parameters on the dryer performance.

The sponge has a spatially uniform porosity ($\varepsilon_{ave} \approx 0.85$) with narrow spaces ($d_{ave} \approx 0.3$ mm) to ensure a uniform moisture content across the material. As sponge is a non-hygroscopic material, so it can be dried completely (*i. e.* final moisture content ≈ zero). However, while conducting initial tests using "sponge" as drying material, it was remarked that the sponge loses water rapidly. Hence, a decision was taken to use "sponge-cotton" as a reference drying material to allow high initial drying and subsequent drying patterns with water holding capability. Experiments are carried out with pre-wetted large sponges placed inside the drying chamber, twelve for every drying shelf.

Ambient air which is sucked by the centrifugal blower, flows to the dryer chamber through the solar air heater where it is preheated. The hot air exiting from the flexible junction

at the lower front portion of the dryer chamber and disperses over the interior space of the dryer chamber and as a result its velocity is reduced. After traveling through and around the drying shelves inside the drying chamber air enters the solar chimney from where it escapes to the surroundings, fig. 1, to achieve uniform drying of wet products.

The temperatures at various locations of the system, solar radiation, relative humidity, and weight loss of drying material are recorded at 1 h interval from 7.00 a. m. in the morning to 7.00 p. m. in the afternoon.

In order to get the sponge initially saturated with water it is necessary to soak it in water and then squeeze-dry it at least twice prior to its final wetting and placement in the shelves. The moisture content is measured by weighting the drying material every 1 h. The drying process is continued till the product achieves its equilibrium (final) moisture content. During each drying experiment, the mass of each specimen on the shelves is measured by removing it from the drying chamber for approximately 25-30 s. The test rig is emptied and recharged with drying specimens each testing day. The experiments are conducted for different air flow rates corresponding to testing days.

Thermal analysis

Evaluation of thermal performance in drying applications is considered a means of assessing how well (or poorly) a dryer operates under the certain conditions.

A thin layer is defined as a thickness of particles [13], in which we can suppose that the airflow parameters (temperature, moisture and velocity) are identical in every point of it.

The drying rate, dM/dt, should be proportional to the difference in moisture content between the material to be dried and the equilibrium moisture content [10]. Mathematically, it can be expressed as thin layer equation:

$$\frac{\mathrm{d}M}{\mathrm{d}t} = -k(M_t - M_e) \tag{1}$$

where M_t and M_e are instantaneous and equilibrium moisture contents and k is the drying rate constant.

The instantaneous moisture content M_t at any given time t on dry basis is computed using the following expression [10]:

$$M_t = \left[\frac{(M_o + 1)W_t}{W_o} - 1\right] \cdot 100\% \tag{2}$$

The weight change over time [10] is used to calculate the moisture change over time. A drying rate constant; k was derived by fitting moisture content and time to a thin layer drying equation of the form:

$$\varphi = \frac{M_t - M_e}{M_o - M_e} = \mathrm{e}^{-kt} \tag{3}$$

where M_0 is the initial moisture content.

The daily overall system drying efficiency, η_d, is a measure of the overall effectiveness of a drying system, including air heater and dryer chamber. It is the ratio of energy required to evaporate the moisture from the product to the energy supplied to the solar dryer; [14, 15], which takes into account the energy consumed by the blower for forced convection solar dryers.

$$\eta_{\mathrm{d}} = \frac{W_v L}{IAt + Q_b} \tag{4}$$

where L is the latent heat of vaporization, W_v [kg] the mass of water content removal, A – the area of dryer, I – the solar radiation, t – the interval of time between two measurements, and Q_{b} – the blower energy delivered to the solar dryer in time, t [kJ].

Results and discussion

The present drying experiments are carried out for solar dryer chamber for five hot summer days of July 2008 in High Institute of Energy, South Valley University, Aswan, Egypt. Each experiment started at 7:00 a. m. and continued until 7:00 p. m. Hourly variation of solar radiation and ambient air temperature in all run days is presented elsewhere [12]. The mean solar radiation and ambient temperature values at the period between the hours 7:00 a. m. and 7:00 p. m. in the five testing days were 645.71 W/m^2 and 41.09 °C, 647.91 W/m^2 and 41.89 °C, 714.39 W/m^2 and 42.06 °C, 659.57 W/m^2 and 43.11 °C, and 717.12 W/m^2 and 43.59 °C with peak values ranging between 1218 W/m^2-1259 W/m^2. The average temperature of the drying air at the inlet of the drying chamber was 65.14 °C. During the experiments, average maximum air temperature in the dryer chamber was 67.7 °C compared to average maximum ambient temperature of 48.05 °C. Mean drying air temperature recorded over the entire test series was 53.68 °C compared with mean ambient temperature of approx. 42.35 °C.

Because of the adequate insulation provided for the duct connecting the air heater and dryer chamber, the difference between the air heater outlet and drying chamber inlet air temperatures is considered negligible.

The variation of solar dryer chamber performance when drying sponge-cotton material with mass flow rate through various runs will be introduced in terms of dimensionless air temperature, moisture ratio, and overall system dryer efficiency. Experimental results showed that the ambient air temperature each day increases till the timing around the noon and after that decreases. Dryer chamber temperature nearly showed the same trend.

Figure 4 shows the dimensionless temperature distribution measured at three vertical positions along section 2 of the drying chamber for specific air mass flow rate $\dot{m}$ = 0.08 kg/s, and different inlet drying air temperatures. Figure 5 illustrates the variation of dimensionless temperature at different sections of dryer chamber shelves at specific mass flow rate and inlet drying air temperature.

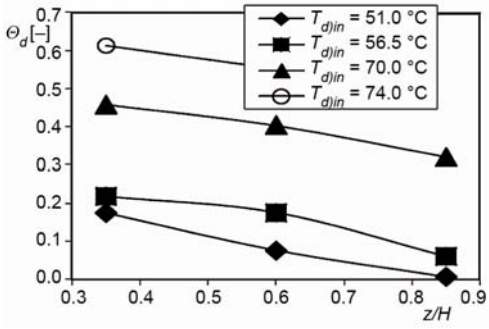

Figure 4. Variation of dimensionless temperature along section 2 of the dryer chamber shelves, $\dot{m}$ = 0.08 kg/s

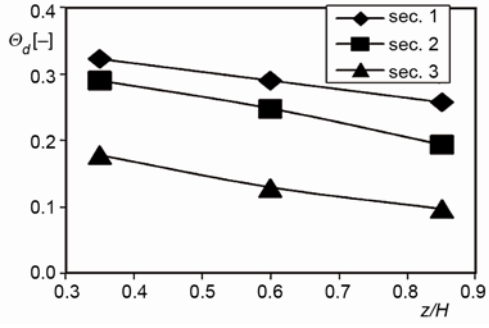

Figure 5. Variation of dimensionless temperature along the dryer chamber shelves, $\dot{m}$ = 0.08 kg/s, $T_{d)in}$ =78.0 °C

The evolution of the temperature within the dryer chamber is the key of the drying phenomenon since an increase of the evaporation rate leads to water content reduction. As it may be expected, the drying material temperature in the beginning of the drying operation is lower than that of drying air. This difference decreases with time. It is apparent that the temperature of the drying air inside the dryer chamber decreases with increasing the height from dryer chamber floor (increasing z). Hence, the lowest temperatures, fig. 4, and highest moisture content, fig. 7, were recorded for locations on the topmost shelf; shelf C. This matches the findings presented in [16]. In addition, fig. 5 illustrates that air temperature decreases as it flows horizontally along the dryer chamber (*i. e.* with increasing x). This may be attributed that, as the hot air moves through the loaded shelves, some of the drying air sensible heat is consumed in evaporation of moisture from the (sponge-cotton) reference drying material, loses its temperature and gains more moisture from the drying product.

It may be concluded from fig. 4 that the amount of increase in the temperature inside the dryer chamber increases with the increment of the dryer chamber air inlet temperature.

However, there is a limit of dryer chamber inlet temperature peak value. As it was mentioned in [17] that increasing the temperature of the drying air will increase the drying rate in two ways. First, this increases the ability of drying air to hold the moisture. Secondly, the heated air will heat the drying sample and increase its vapor pressure. This will drive the moisture to the surface faster. A high drying air temperature could also result in more heat loss by conduction and radiation from both the air heater and dryer chamber, resulting in overall reduction in system efficiency. Results for one mass flow rate are presented since the other mass flow rates exhibit similar trends.

Drying parameters have been recorded at different dryer chamber shelves. It was found that there were significant variations in drying parameters at different shelves during the drying period.

Figure 6 presents the moisture ratio *vs.* drying time for various drying shelves. It may be shown from the figure that the moisture content decreased rapidly nearly half the drying time interval and continued to fall but at a reduced rate approaching the equilibrium moisture content. This might be attributed to that the rate of water removal decreases with the decrease in moisture content of drying product during this period. Hence, its ability to absorb heat and temperature rise decreases and that hot air might immigrates through the dryer chamber before flowing outside through the chimney. The present work nearly have the same trend with that presented in [10]. A detailed comparison of the trends obtained in this study with those for previously reported in [10] is not appropriate owing to variations in climatic conditions (particularly solar radiation variations which have been shown to affect strongly the drying air temperatures) in both investigations.

Further, it may be remarked from fig. 6 that shelf moisture ratio increases with vertical distance, owing to the evaporation of water from the wet material in the lower shelves.

The weight change over time is used to calculate the variation of moisture ratio with dryer chamber inlet temperature. It may be remarked from fig. 7 that the moisture ratio decreases from the maximum value (= 1.0) at 7:00 a. m. at which the dryer chamber inlet temperature is 45 °C with increasing dryer chamber inlet temperature until it reaches around 82 °C (indicating weight loss about 80%). The plots indicate that the moisture ratio continues to decrease with a slower rate until finally approaching the equilibrium moisture content ($\varphi \approx 0$) at dryer chamber inlet chamber of 59.7 °C at 7:00 p. m. These findings match the observations mentioned in [10, 11].

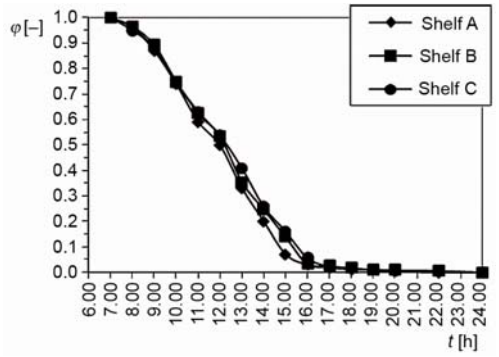

Figure 6. Variation of moisture ratio for different shelves with drying time, $\dot{m}$ = 0.048 kg/s

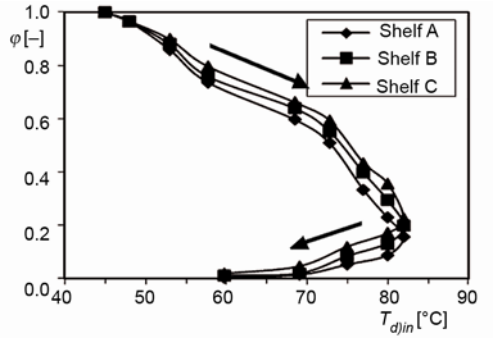

Figure 7. Variation of shelves moisture ratios with dryer chamber inlet temperature; $\dot{m}$ = 0.064 kg/s

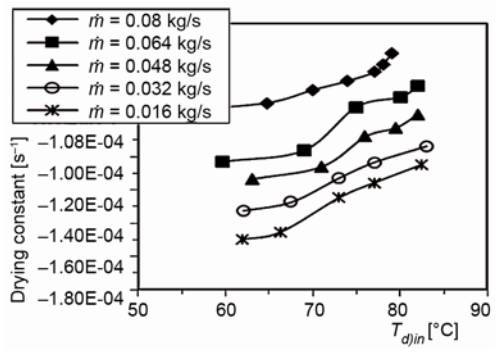

Figure 8. Variation of drying constant, *k*, with dryer chamber inlet temperature for various air mass flow rates

Figure 8 presents the variation of drying constant; *k* determined from experimental data, with dryer chamber inlet temperature for different air mass flow rates. Drying constant is nearly constant during the initial period and increases with the increase of dryer chamber inlet temperature. It was indicated in [11] that drying constant change may be due to the increase in thickness of the water layer in the micro-pores with an increase in moisture content. Also, it may be due to the water removal, which occurs in different layers of the drying product during the drying.

The performance evaluation of the drying system is also represented by overall (overall indicates both air heater & dryer chamber) efficiency of the solar drier. Overall efficiency is a measure of the capacity of the heated air to remove the moisture from the products.

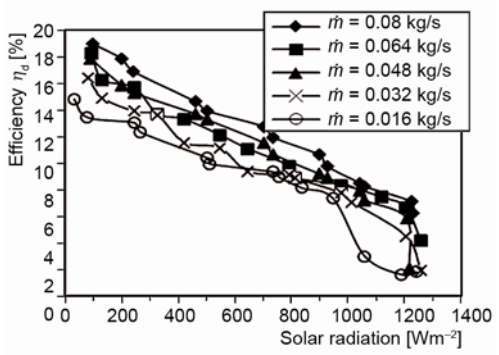

Figure 9. Overall efficiency variation with solar radiation for different mass flow rates

As it was indicated in [18], overall efficiency of a drying device is related to many factors such as the physical and chemical properties of dried materials, the drying characteristics of the dried materials, the time in the drying process, climatic conditions and structure of the drying devices.

Figure 9 presents the variation of overall efficiency of the solar drier for drying sponge-cotton reference drying material with solar radiation for different mass flow rates. All efficiency curves presented in fig. 9 are nearly similar in shape. In the early stage, drying is relatively easy and therefore, a high overall efficiency value is obtained and in the later stage, a decrease in overall efficiency is obtained due to the decrease in moisture content in the product. This matches the findings presented in

[10]. As the solar radiation increases, the temperature of the air entering the drying chamber increases, leading to subsequent increase of the temperature within the dryer chamber, hence, water content of the material to be dried reduces and the efficiency of the dryer decreases.

As it was indicated in [4], the overall efficiency is significantly improved by high air flow rates. This may be attributed to the increase of the contact between the drying product and air.

It may be remarked that the overall efficiency varies between 18.6 and 1.85%. These results indicate that the overall efficiency of the solar drying of the reference drying material was very low.

As it was indicated earlier that drying air temperature is the predominant factor affecting the drying quality. Another factor affecting the drying quality is the drying rate.

It is evident from figs. 10 and 11 that dryer chamber inlet temperature and air mass flow rate have remarked influence on drying rate. It can be seen that the drying rate is not constant throughout the drying period and that drying curves show a short period of slow drying rate change followed by a long period of steep drying rate change. This matches the findings listed in [18, 19]. Further, it may be remarked that a higher drying air temperature produced a higher drying rate (figs. 10 and 11) with subsequent decrease in moisture ratio. As it was indicated in [20], this may be due to the increase of the air heat supply rate to the drying product and the subsequent acceleration of water migration inside it.

As one might expect, shelf A; which is the one placed nearer to air inlet, exhibits the most rapid drying than the two higher shelves B and C. This may be attributed to that the bottom shelf receives the greatest heat supply from the incoming hot air from the solar air heater, while the top shelf receives a reduced amount of heat supply as well as cooler and more humid air. This matches the findings presented in [7].

As it was indicated in [21] that drying rate is case sensitive, although rapid drying rate is required to ensure safe storage moisture content is reached before product decay processes start, however, product case hardening may occur if the drying proceeds too rapidly.

Figure 11 shows that the drying rate increases with the increase of drying air flow rate leading to subsequent decrease of the drying time. As it was listed in [10], this may be attributed to the interaction of large volume of air with the drying product and the acceleration of the moisture migration inside the dryer chamber.

The uncertainty in a result is calculated on the basis of the uncertainties in the measurements of all the related independent variables [22]. An uncertainty analysis is performed, and the uncertainty in overall efficiency of the drying system is found to be ±4.27%.

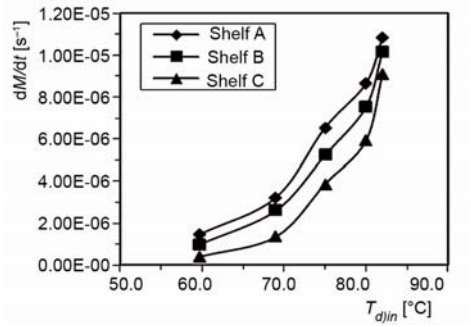

Figure 10. Variation of drying rate along dryer chamber shelves with dryer chamber inlet temperature; $\dot{m}$ = 0.064 kg/s

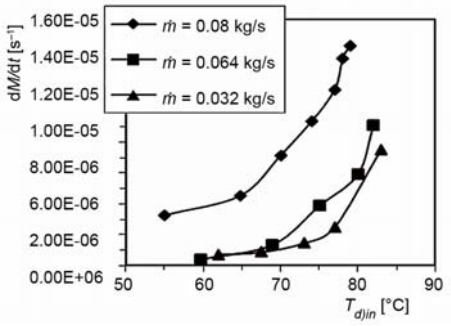

Figure 11. Variation of drying rate along dryer chamber (shelf C) with dryer chamber inlet temperature for various mass flow rates

Empirical correlations and corresponding values of coefficient of determination for temperature change across dryer chamber and moisture ratio *v. s*. dryer chamber inlet temperature are evaluated to give an insight of the drying curves of sponge-cotton material.

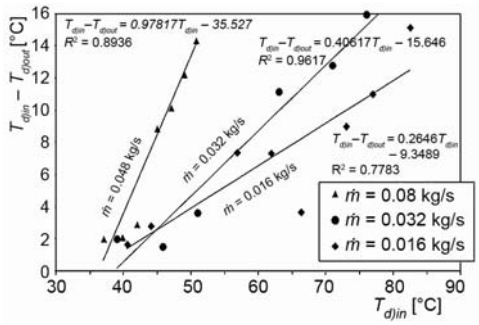

Figure 12. Variation of temperature decay across the dryer chamber with dryer chamber inlet temperature

Variation of temperature change across the dryer chamber with dryer chamber inlet temperature for different mass flow rates is shown in fig. 12. Linear correlations are used to fit the experimental data. It may be remarked from the figure that the data are scattered. It is not possible to present the temperature lapse across the dryer chamber, for different air mass flow rates and drying air temperatures by a single curve. As seen from fig. 12, different linear equations will be utilized to curve fit the experimental data corresponding to different mass flow rates. It may be shown from fig. 12, as might be expected, that for a specific mass flow rate, the temperature lapse in the dryer chamber increases with increasing dryer chamber inlet temperature and that for specific dryer chamber inlet temperature, the temperature lapse across the dryer camber increases as the air mass flow rate increases. Further, investigation is required to ensure that interpolation may be utilized to evaluate the temperature lapse rates for intermediate mass flow rates.

The effect of dryer chamber inlet temperature on mean value of moisture ratio, before and after sun noon, is shown in fig. 13. Second-order polynomial equations fit experimental data are shown in the figure. As, it may be expected that the moisture ratio, before sun noon, decreases with time *i. e.* with increasing dryer chamber inlet temperature. This is due to the increase of the air heat supply rate and the acceleration of water migration in different layers of drying material during drying process. After sun noon, *i. e.* with decreasing dryer chamber inlet temperature, moisture ratio continues to decrease. This might be attributed to the thermal inertia of the system.

The variation of logarithm of mean value of moisture ratio, lnφ, with drying time is presented in fig. 14. Correlations between lnφ and drying time for the current investigation and that for Shanmugam and Natarajan [10] are plotted in the figure. It is apparent from figs. 13 and 14 that moisture ratio decreases continuously with drying time.

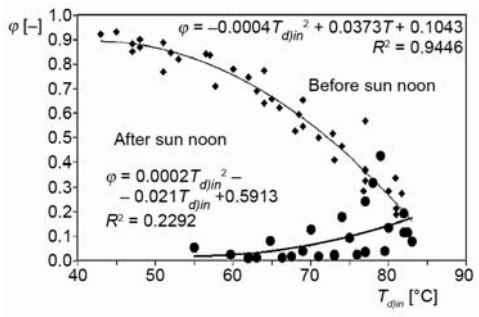

Figure 13. Mean value of moisture ratio, φ, in dryer chamber *vs*. dryer chamber inlet temperature variation

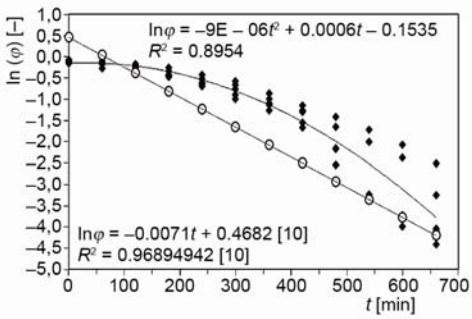

Figure 14. Variation of logarithm of mean value of moisture ratio, lnφ with drying time

It may be remarked from fig. 14 that there is reasonably close agreement between $\ln\varphi$ for the current investigation and that for Shanmugam and Natarajan [10] and that the difference is low in the morning and evening periods as compared to the afternoon where dryer chamber inlet temperature was high. The discrepancy between $\ln\varphi$ for the two investigations might be attributed to the variations in dryer design, construction materials, and operating conditions.

Conclusions

On the basis of the experimental results obtained for five testing days in an indirect type forced convection solar dryer manufactured and tested in High Institute of Energy, South Valley University, Aswan, Egypt, the following conclusions can be drawn.

- The temperature of the drying air inside the chamber decreases as it flows horizontally and vertically along the dryer chamber.
- There were significant variations in drying parameters at different shelves during the drying period.
- The moisture ratio decreases from the maximum value (= 1.0) at 7:00 a. m. at which the dryer chamber inlet temperature is nearly 45 °C with increasing dryer chamber inlet chamber.
- The moisture ratio increases with vertical distance owing to evaporation of water from the wet material in the lower shelves.
- Drying air temperature is the main factor in controlling the drying performance and that higher drying air temperature produced higher drying rate and more temperature decay across the dryer chamber.
- Drying constant was nearly constant during the initial drying period and increases with the increase of dryer chamber inlet temperature.
- The overall efficiency and drying rate increase with the increase of drying air flow rate leading to subsequent decrease of the moisture ratio and drying time.
- Maximum overall efficiency of 18.6% was observed for air mass flow rate of 0.08 kg/s.
- Linear equations will be utilized to curve fit the temperature lapse in the dryer chamber for different mass flow rates.
- Second-order polynomial equations fit mean value of moisture ratio variation with dryer chamber inlet temperature.

Nomenclature

A – cross-sectional area of the dryer, [m^2]
H – dryer chamber height, [m]
I – solar radiation, [Wm^{-2}]
k – drying rate constant, [s^{-1}]
L – latent heat of vaporization, [$kJkg^{-1}$]
Q_b – blower energy delivered to the solar dryer in time, t, [kJ]
M_e – equilibrium moisture content, [kg water/kg dry matter]
M_f – final moisture content, [kg water/kg dry matter]
M_o – initial moisture content, [kg water/kg dry matter]
M_t – moisture content at any time of drying, [kg water/kg dry matter]
$\dot{m}$ – air mass flow rate [kgs^{-1}]
dM/dt – drying rate at any time of drying [kg water/kg dry matters]
R^2 – coefficient of determination, [–]
T – temperature, [K]
t – time, [s]
W_o – mass of material to be dried at $t = 0$, [kg]
W_t – mass of material to be dried at any time t, [kg]
W_v – mass of water content removal, [kg]
x – horizontal distance along the dryer, [m]
z – vertical distance along the dryer, [m]

Greek symbols

η_d – overall efficiency of drying system, [–]
φ – moisture ratio, [–]
θ – dimensionless temperature, [$= (T - T_o)/(T_{in} - T_o)$], [–]

Subscripts

amb – ambient
ave – average
d – dryer chamber
in – inlet
out – outllet

References

[1] Saim, R., *et al*., Computational Analysis of Transient Turbulent Flow and Conjugate Heat Transfer Characteristics in a Solar Collector Panel with Internal Rectangular Fins and Baffles, *Thermal Science, 14* (2010), 1, pp. 221-234
[2] Dragićević, S. M., Lambić, M. R., Numerical Study of a Modified Trombe Wall Solar Collector System, *Thermal Science*, *13* (2009), 1, pp. 195-204
[3] Stefanović, V. P., Bojić, M. Lj., Development and Investigation of Solar Collectors for Conversion of Solar Radiation into Heat and/or Electricity, *Thermal Science*, *10* (2006), 4, pp. 177-187
[4] Ekechukwu, O. V., Norton, B., Review of Solar-Energy Drying Systems II: an Overview of Solar Drying Technology, *Energy Conversion & Management*, *40* (1999), 6, pp. 615-655
[5] Thanvi, K. P., Pande, P. C., Development of a Low-Cost Solar Agricultural Dryer for Arid Regions of India, *Energy in Agriculture*, *6* (1987), 1, pp. 35-40
[6] Esper, A., Muhlbauer, W., Solar Drying – An Effective Means of Food Preservation, *Renewable Energy*, *15* (1998), 1-4, pp. 95-100
[7] El-Sebaii, A. A., *et al*., Experimental Investigation of an Indirect Type Natural Convection Solar Dryer, *Energy Conversion and Management*, *43* (2002), 16, pp. 2251-2266
[8] Ramana Murthy, M. V., A Review of New Technologies, Models and Experimental Investigations of Solar Driers, *Renewable and Sustainable Energy Reviews*, *13* (2009), 4, pp. 835-844
[9] Tiris, C., *et al*., Experiments on a New Small-Scale Solar Dryer, *Applied Thermal Engineering*, *16* (1996), 2, pp. 183-187
[10] Shanmugam, V., Natarajan, E., Experimental Investigation of Forced Convection and Desiccant Integrated Solar Dryer, *Renewable Energy*, *31* (2006), 8, pp. 1239-1251
[11] Kadam, D. M., Samuel, D. V. K., Convective Flat-Plate Solar Heat Collector for Cauliflower Drying, *Biosystems Engineering*, *93* (2006), 2, pp. 189-198
[12] Aissa, W., *et al*., An Experimental Investigation of Forced Convection Flat Plate Solar Air Heater with Storage Material, *Thermal Science, 16* (2012), 4, pp. 1205-1216
[13] Khiari, B., *et al*., Experimental and Numerical Investigations on Water Behavior in a Solar Tunnel Drier, *Desalination*, *168* (2004), pp. 117-124
[14] Arinze, E. A., *et al*., Design and Experimental Evaluation of a New Commercial Type Mobile Solar Grain Dryer Provided with High Efficiency Fined-Plate Collector, *Renewable Energy*, *9* (1996), 1-4, pp. 670-675
[15] Arinze, E. A., *et al*., Design and Experimental Evaluation of a Solar Dryer for Commercial High Quality-Hay Production, *Renewable Energy*, *16* (1999), 1-4, pp. 639-642
[16] Vlachos, N. A., *et al*., Design and Testing of a New Solar Tray Dryer, *Drying Technology*, *20* (2002), 5, pp. 1239-1267
[17] Augustus Leon, M., *et al*., A Comprehensive Procedure for Performance Evaluation of Solar Food Dryers, *Renewable and Sustainable Energy Reviews*, *6* (2002), 4, pp. 367-393
[18] Li, Z., *et al*., Experimental Investigation on Solar Drying of Salted Greengages, *Renewable Energy*, *31* (2006), 6, pp. 837-847
[19] Karim, M. A., Hawlader, M. N. A., Mathematical Modelling and Experimental Investigation of Tropical Fruits Drying, *International Journal of Heat and Mass Transfer*, *48* (2005), 23-24, pp. 4914-4925
[20] Lahsasni , S., *et al*., Drying Kinetics of Prickly Pear Fruit (*Opuntia ficus indica*), *Journal of Food Engineering*, *61* (2004), 2, pp. 173-179
[21] Ekechukwu, O. V., Norton, B., Experimental Studies of Integral-Type Natural-Circulation Solar-Energy Tropical Crop Dryers, *Energy Convers. Mgmt., 38* (1997), 14, pp. 1483-1500
[22] Figliola, R. S., Beasley, D. E., *Theory and Design for Mechanical Measurements*, 2nd ed., John Wiley & Sons, New York, USA, 1995

Paper submitted: July 10, 2011
Paper revised: May 22, 2012
Paper accepted: May 25, 2012